Available online at www.sciencedirect.com

Polyhedron 23 (2004) 969–978

POLYHEDRON

www.elsevier.com/locate/poly

Synthesis, EPR and Mössbauer spectral studies of new iron(III) complexes with 2-benzoylpyridine-N(4), N(4)-(butane-1,4-diyl) thiosemicarbazone (HBpypTsc): X-ray structure of $[Fe(BpypTsc)_2]FeCl_4 \cdot 2H_2O$ and the free ligand

Anandaram Sreekanth [1], M.R. Prathapachandra Kurup *

Department of Applied Chemistry, Cochin University of Science and Technology, Kochi 682 022, Kerala, India

Received 11 August 2003; accepted 9 December 2003

Abstract

Three novel iron(III) complexes of 2-benzoylpyridine N(4), N(4)-(butyl-1,4-diyl) thiosemicarbazone (HBpypTsc), $[Fe(BpypTsc)_2]ClO_4$ (**1**), $[Fe(BpypTsc)_2]NO_3$ (**2**) and $[Fe(BpypTsc)_2]FeCl_4$ (**3**) were synthesized and physico-chemically characterized by means of partial elemental analyses, magnetic measurements (polycrystalline state), UV–Vis and IR spectroscopies. The spin Hamiltonian parameters, isomer shifts and quadrupolar splitting values of the complexes were assigned by variable temperature EPR and Mössbauer spectra. The presence of a spin-paired iron(III) cation with $d_{xz}^2 d_{yz}^2 d_{xy}^1$ ground state is revealed by the simulated EPR spectral data. The structures of the free ligand HBpypTsc and one of the complexes $[Fe(BpypTsc)_2]FeCl_4$ (**3**) were solved by single crystal X-ray diffraction which authenticated a FeN_4S_2 octahedral coordination in the complex, as envisaged from the spectral data. All complexes except $[Fe(BpypTsc)_2]FeCl_4$ (**3**) were found to be low-spin $S = 1/2$ ($^2T_{2g}$), whereas **3** was found to have both low-spin ($^2T_{2g}$) and high-spin ($^6A_1$) centres.

Keywords: Iron(III) complexes; Thiosemicarbazone; Single crystal X-ray diffraction; Mössbauer spectra; EPR spectra; IR spectra

1. Introduction

The discovery of a low-spin ($S = 1/2$) non-heme $[Fe^{III}N_2S_3]$ centre in the enzyme nitrile hydratase has raised interest in mononuclear model iron(III) complexes with N, S coordination [1,2]. Several groups have structurally characterized iron(III) complexes with N_xS_y coordination and compared their spectroscopic properties with the biological iron site [3,4]. The well-documented biological activities of several heterocyclic thiosemicarbazones have often attributed to a chelation phenomenon with transition metal ions [5]. The success in therapeutic applications of N-heterocyclic thiosemicarbazones for removing excess iron from iron-loaded mice through chelation therapy is quite remarkable [6]. We have previously examined the chelation behavior of some O–N–S and N–N–S donor thiosemicarbazones with several transition metal ions with the aim of gaining more information about their nature of coordination and related structural, spectral and biological properties [7–11]. There are some interesting reports on the iron(III) complexes of biologically active 2-acetylpyridine thiosemicarbazones [12,13]. This paper discusses the syntheses and spectral studies of three iron(III) complexes with the title ligand 2-benzoylpyridine N(4), N(4)-(butane-1,4-diyl)thiosemicarbazone (HBpypTsc) (Scheme 1). A previously reported complex of a 2-acetylpyridine thiosemicarbazone prepared from $FeCl_3$, gave a stoichiometry $FeLCl_2$ which suggested it to be a five-coordinate iron(III) complex having an

---

* Corresponding author. Tel.: +91-484-2575804; fax: +91-484-2577595.

E-mail addresses: sran@esr.phys.chem.ethz.ch (A. Sreekanth), mrp@cusat.ac.in (M.R.P. Kurup).

[1] Present address: Laboratorium für Physikalische Chemie, Eidgenössische Technische Hochschule, Honggerberg, CH-8093, Zurich, Switzerland. Tel.: +41-1-6325702; fax: +41-1-6321538.

0277-5387/$ - see front matter © 2004 Elsevier Ltd. All rights reserved.
doi:10.1016/j.poly.2004.01.006

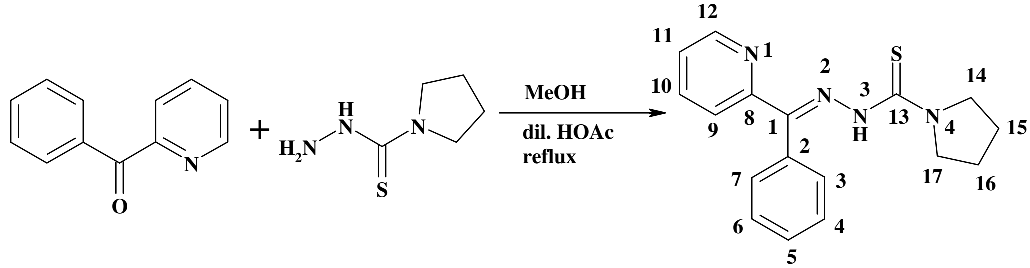

Scheme 1.

intermediate spin state [14]. However the structural information as well as the spectral information obtained for a similar compound, **3** in our case, confirmed that the previous report could be incorrectly formulated.

2. Experimental

2.1. General

2-Benzoylpyridine (Lancaster), ferric chloride (Merck) and ferric nitrate (Merck) was used as received. Ferric perchlorate was prepared from ferric carbonate by digesting it with perchloric acid followed by evaporating the solution on a sand bath followed by subsequent cooling. *Caution! Perchlorate salts are potentially explosive and should be handled with care.* Pyrrolidine-1-thiocarboxylic acid hydrazide was synthesized by adopting and modifying a reported procedure [15]. All solvents were distilled before use.

2.2. Synthesis of HBpypTsc

To a solution of pyrrolidine-1-thiocarboxylic acid hydrazide (0.1 mol) and 2-benzoylpyridine (0.1 mol) in 20 mL methanol, 2 drops of conc. acetic acid was added and the reaction mixture was heated under reflux for 5 h. The reaction mixture was kept for 3 days where the deep yellow colored crystals of HBpypTsc began to separate in a decent yield with satisfactory analytical data. X-ray quality single crystals of the compound were grown from a solution of the compound HBpypTsc in chloroform layered with methanol in 3 days. Melting point 185–186 °C. ^{1}H NMR δ (ppm): NH, 14.3, singlet 1H; 8.73, doublet, aromatic, 1H, $J = 7.5$ Hz; 8.5, aromatic, doublet, 1H; 7.1–7.8, aromatic, multiplet, 7H, 3.8, aliphatic, multiplet, 4H, 1.9, aliphatic, multiplet, 4H.

2.3. Synthesis of [Fe(BpypTsc)$_2$]ClO$_4$ (*1*)

To a methanolic solution of ferric perchlorate (1 mmol) was added a solution of HBpypTsc (2 mmol) in chloroform and the mixture was refluxed for 30 min. The resulting deep green colored solution was evaporated to half its volume. On cooling dark brown shining crystals of compound **1** separated out and were washed with ether and dried over P_4O_{10} in vacuo.

2.4. Synthesis of [Fe(BpypTsc)$_2$]NO$_3$ (*2*)

To a methanolic solution of ferric nitrate (1 mmol) was added a solution of HBpypTsc (2 mmol) in chloroform and the mixture was refluxed for 30 min. The resulting deep green colored solution was evaporated to half of its volume. On cooling dark brown shining crystals of compound **2** separated out and were washed with ether and dried over P_4O_{10} in vacuo.

2.5. Synthesis of [Fe(BpypTsc)$_2$]FeCl$_4$ (*3*)

To a methanolic solution of ferric chloride (1 mmol) was added a solution of HBpypTsc (1 mmol) in chloroform and the mixture was refluxed for 30 min. The resulting deep green colored solution was evaporated to half its volume. On cooling dark brown shining crystals of compound **3** separated out and were washed with ether and dried over P_4O_{10} in vacuo. X-ray quality single crystals of the compound were grown by the slow evaporation of a methanolic solution of the complex in 7 days.

2.6. Physical methods

Microanalyses were carried out using a Heraeus Elemental Analyzer at CDRI, Lucknow, India. Infrared spectra were recorded on a Shimadzu DR 8001 series FT-IR instrument as KBr pellets in the range 400–4000 cm^{-1} and far-IR spectra were recorded in the range 50–500 cm^{-1} on a NICOLET MAGNA 550 FT-IR spectrometer using polyethylene pellets at RSIC, IIT, Bombay, India. Electronic spectra were recorded in the 900–250 nm range in a diffused reflectance mode in MgO matrix in Ocean Optics SD 200 fiber optic Spectrophotometer. Magnetic measurements were made in the polycrystalline state on a home built simple Gouy balance using Hg[Co(SCN)$_4$] as calibrant. EPR spectra were recorded in a Bruker ESP300, X-band CW spectrometer operating at 9.52 GHz equipped with a liquid

Table 1
Crystal data and structure refinement parameters

	HBpypTsc	[Fe(BpypTsc)$_2$]FeCl$_4 \cdot 2$H$_2$O (**3**)
Empirical formula	$C_{17}H_{18}N_4S$	$C_{34}H_{38}Cl_4Fe_2N_8O_2$ S_2
Formula weight, *M*	310.41	908.34
Temperature, *T* (K)	298(2)	293(2)
Wavelength, Mo Kα (Å)	0.70930	0.70930
Crystal system	orthorhombic	triclinic
Space group	$P2_1P2_1P2_1$	$P\bar{1}$
Unit cell dimensions		
a (Å)	9.95	9.64
b (Å)	10.77	15.15
c (Å)	14.89	16.24
α (°)	90.00	114.57
β (°)	90.00	93.79
γ (°)	90.00	101.76
Volume, *V* (Å^3)	1596.3	2082.1
Z, Calculated density, ρ (Mg m^{-3})	4, 1.292	2, 1.449
Absorption coefficient, μ (mm^{-1})	0.205	1.094
F(000)	656	932
Crystal size (mm)	$0.35 \times 0.35 \times 0.30$	$0.275 \times 0.175 \times 0.150$
θ Range for data collection	2.33–24.90	1.40–24.92
Limiting indices	$0 \leqslant h \leqslant 11$, $0 \leqslant k \leqslant 12$, $0 \leqslant l \leqslant 17$	$0 \leqslant h \leqslant 11$, $-17 \leqslant k \leqslant 17$, $-19 \leqslant l \leqslant 19$
Reflections collected/Unique	1526/1526 [$R_{\text{int}} = 0.000$]	5912/5912 [$R_{\text{int}} = 0.000$]
Completeness to 2θ (°, %)	24.90, 94.1	24.92, 80.8
Maximum and minimum transmission	1.000 and 0.989	1.000 and 0.969
Goodness-of-fit on F^2	1.075	1.134
Final *R* indices [$I > 2\sigma(I)$]	$R_1 = 0.0332$, $wR_2 = 0.0777$	$R_1 = 0.0605$, $wR_2 = 0.1535$
R indices (all data)	$R_1 = 0.0387$, $wR_2 = 0.0825$	$R_1 = 0.0895$, $wR_2 = 0.1726$
Largest difference peak and hole (e Å^{-3})	0.174 and −0.224	1.287 and −0.405

nitrogen cryostat. The spectra were measured with a modulation amplitude of 0.05(0.1) mT and 100 kHz modulation frequency, and the field was calibrated by using 2,2-diphenyl-1-picrylhydrazyl (DPPH) with a *g* value of 2.0036. NMR spectra were recorded on a Bruker DRX 500 instrument using $CDCl_3$ as the solvent and TMS as the internal reference at the Sophisticated Instruments Facility, Indian Institute of Science, Bangalore, India. The tentative structure of the compound HBpypTsc was assigned on the basis of different NMR experiments, based on the couplings and connectivities of the signals observed. The ^{1}H resonances were assigned on the basis of chemical shifts, multiplicities and coupling constants from ^{1}H NMR experiments. The assignments of the NH and OH hydrogens were made by comparison with the spectra recorded on deuterium exchange. The carbon types were determined by ^{13}C-Spin Echo Fourier Transform (SEFT) experiments. Mössbauer spectra were recorded on a constant-acceleration spectrometer with multi channel analyzer using a ^{57}Co source in a Rhodium matrix at Inter University Consortium, Indore, India.

2.7. X-ray crystallography

A dark brown triclinic crystal of the [Fe(BpypTsc)$_2$]-FeCl$_4$ (**3**) and a deep yellow orthorhombic crystal of HBpypTsc having appropriate dimensions were sealed in a glass capillary, and intensity data were measured at room temperature (293 K) on an Nonius MACH3 diffractometer equipped with graphite-monochromated Mo Kα ($\lambda = 0.71073$ Å) radiation. The trial structure was obtained by direct methods using SHELXL-97 and refined by full-matrix least squares on F^2 (SHELXS-97) [16,17]. The non-hydrogen atoms were refined with anisotropic thermal parameters. All hydrogen atoms were geometrically fixed and allowed to refine using a riding model. Absorption corrections were employed using ψ-scan. The crystallographic data along with details of structure solution refinements are given in Table 1.

3. Results and discussions

3.1. Syntheses

The ligand HBpypTsc was synthesized by a direct condensation of the ketone with the thiosemicarbazide. In the ^{1}H NMR spectrum the signal for N(2)H is observed at a low field of $\delta = 14.35$ ppm and this signal disappears on deuterium exchange, which is consistent with the Z configuration of the thiosemicarbazone moiety. The low frequency multiplets at $\delta = 3.8$ (4H) and 1.9 (4H) ppm were attributed to pyrrolidine ring protons C14 and C15, respectively, which are chemically and magnetically equivalent with C17 and C16 (the numbering scheme of HBpypTsc is given in Scheme 1). Aromatic protons of the pyridine and phenyl ring appear at $\delta = 8.73$, doublet, aromatic, 1H, $J = 7.5$ Hz; 8.5, aromatic, doublet, 1H and 7.1–7.8, aromatic, multiplet, 7H, respectively. The carbon atoms were assigned on the basis of proton decoupled ^{13}C and ^{13}C- Spin Echo Fourier Transform NMR spectra. Eighteen signals were observed in the ^{13}C NMR spectrum, which are assigned as follows. Signals at $\delta = 177.0$ and 177.6 ppm were attributed to C(1)=N(2) and C(13)=S(1) of the thiosemicarbazone moiety. Aromatic carbons of the pyridine and phenyl ring of the 2–benzoylpyridine moiety appear at $\delta = 121.5$ (C5), 123.8 (C4), 126.1 (C6), 128.4 (C10), 129.2 (C11), 129.6 (C3), 129.9 (C9), 137.3 (C7), 143.9 (C2), 148.0 (C9), 149.2 (C12), 152.8 (C8), whereas the peaks at $\delta = 53.4$, 50.4, 26.6 and 24.3 were assigned to aliphatic carbons C14, C17, C15 and C16, respectively, of the pyrrolidine ring.

All complexes were dark brown and are readily soluble in polar organic solvents. Their stoichiometries and partial elemental analysis data are shown in Table 2. Analytical data shows a 1:2:1 ratio of iron, ligand and anions for FeL$_2$X [X = ClO$_4$, FeCl$_4$$^-$, NO$_3$]. From the analytical data obtained for compound **3** two formulations are possible: [Fe(BpypTsc)$_2$]FeCl$_4$ or [FeBpypTscCl$_2$], but from the crystallographic as well as the spectroscopic data it is clear the compound isolated is the former one consisting of an ion pair. The compounds were 1:1 electrolytes [18] in DMF with Λ_m values near to 95 Ω^{-1} cm^2 mol^{-1}. The cation centre of all the complexes are expected to contain two deprotonated ligands attached to an iron(III) centre. Magnetic moments have been determined for all the complexes at room temperature in the polycrystalline state. Iron(III) is known to exist in three states with $S = 5/2$ (^{6}A$_1$, $\mu = 5.92$ BM), 3/2 (^{4}A$_2$, $\mu = 3.87$ BM) and 1/2 (^{2}T$_2$, $\mu = 1.73$ BM)[19]. The magnetic moments of the compounds **1** and **2** are 1.89 and 2.33 BM, respectively, indicating these compounds are typical low spin compounds. The high values of susceptibility for compound **3** indicate the presence of a high spin centre in the molecule [20,21]. The complete assignment of the spin states of the complexes were done on the basis of EPR and Mössbauer measurements.

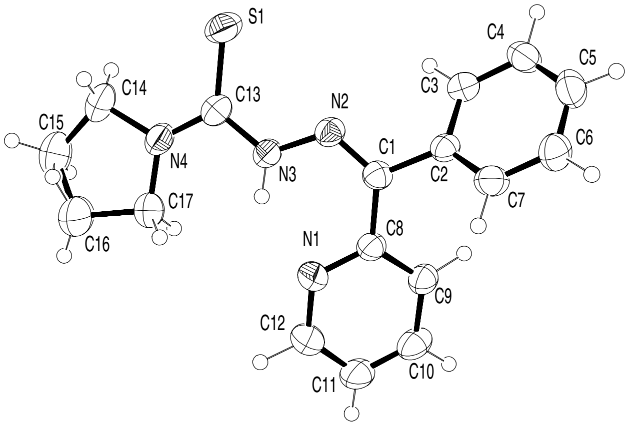

Fig. 1. ORTEP diagram of the compound HBpypTsc, with 54% ellipsoidal probability. Hydrogen atoms are shown as smaller spheres of arbitrary radii.

3.2. Molecular and crystal structure of compound HBpypTsc

Fig. 1 shows the molecular structure of the compound along with the atom numbering scheme. The molecule exists in the E conformation around the N2–N3 bond. The structure reveals quasicoplanarity in the plain of the thiosemicarbazone but both the aromatic rings are bifurcated. The molecular structure reveals that the compound exists in the thione form. Table 3 illustrates selected bond lengths and angles.

The compound has two double bonds in the thiosemicarbazone moiety viz. C1–N2 1.295 Å and C13–S1 1.681 Å which are consistent with the previously reported cases. The planarity in the thiosemicarbazone is revealed by a smaller dihedral angle of the N2–N3–C13–S1 (0.9°) skeleton. A considerable amount of ring bifurcation from the plane of the thiosemicarbazone is indicated by the dihedral angles C1–N2–N3–C13 (−176.9°) and C8–C1–C2–C7 (−44.7°). The S and pyridyl N1 atoms are in E configuration with respect to the C1–N2 bond. The five-membered pentamethyleneimine (pyrrolidine) ring is not planar and tends towards an envelope conformation [22]. The smaller dihedral angles between the pyridyl ring and the phenyl ring of the 2-benzoylpyridine moiety and thiosemicarbazone moiety C2–C1–C8–C9 (−28.2°) and N3–N2–C1–C8 (2.2°), is due to a resonance effect between the π systems. Pyridyl nitrogen N1 is intramolecularly hydrogen bonded to

Table 2
Stoichiometries and partial elemental analysis of the complexes

Compounds	Stoichiometries	*Anal.* Calc. (Found) (%)			μ (BM)
		C	H	N	
[Fe(BpypTsc)$_2$]ClO$_4$ (**1**)	C$_{34}$H$_{34}$ClFeN$_8$O$_4$S$_2$	52.74 (52.75)	4.40 (4.43)	14.45 (14.48)	1.89
[Fe(BpypTsc)$_2$]NO$_3$ (**2**)	C$_{34}$H$_{34}$FeN$_9$O$_3$S$_2$	55.40 (55.43)	4.65 (4.65)	17.09 (17.11)	2.33
[Fe(BpypTsc)$_2$]FeCl$_4$ (**3**)	C$_{34}$H$_{34}$Cl$_4$Fe$_2$N$_8$S$_2$	46.80 (46.81)	3.93 (3.93)	12.85 (12.85)	4.38

Table 3
Selected bond lengths (Å) and angles (°) of HBpypTsc

Bond lengths		Bond angles	
S(1)–C(13)	1.681(3)	C(1)–N(2)–N(3)	118.4(2)
N(1)–C(12)	1.341(4)	C(13)–N(3)–N(2)	121.1(2)
N(1)–C(8)	1.342(4)	N(1)–C(8)–C(9)	121.7(3)
N(2)–C(1)	1.295(4)	N(1)–C(8)–C(1)	117.5(2)
N(2)–N(3)	1.366(3)	N(1)–C(12)–C(11)	123.9(4)
N(3)–C(13)	1.360(4)	N(3)–C(13)–S(1)	124.0(2)
X–H···Cg	H···Cg (Å)	X···Cg (Å)	∠X– H···Cg (°)
C12–H12···Cg(3)[a]	2.8518	3.6071	126.85
C16–H16···Cg(2)[b]	3.2937	4.1282	145.44
D–H···A	H···A (Å)	D···A (Å)	∠D–H···A (°)
N3–H103···N1[c]	1.94	2.659	136
C11–H11···N2[c]	2.59	3.409	153

Cg(2) = N1, C8, C9, C10, C11, C12; Cg(3) = C2, C3, C4, C5, C6, C7.
Cg, centroid; D, donor and A, acceptor.

[a] Equivalent position code: $1/2 - x, 1 - y, 1/2 + z$.

[b] Equivalent position code: $1 - x, -1/2 + y, 1/2 - z$.

[c] Equivalent position code: x, y, z.

N3–H10 at 2.65 Å distance forming a six-membered ring.

3.3. Molecular and crystal structure of compound 3

The compound $Fe(BpypTsc)_2FeCl_4 \cdot 2H_2O$ (**3**) crystallizes with two molecules of water of crystallization. Table 4 presents the selected bond lengths and angles. Fig. 2 shows the molecular structure of the compound along with the atom numbering scheme. The low-spin iron(III) ion has a distorted octahedral geometry in the complex. The pattern of coordination is similar to that observed in similar types of complexes [23]. The two molecules of monodeprotonated ligand, coordinate to iron via pyridyl nitrogens, azomethine nitrogens and thiolato sulfur atoms to form four five membered che-

Table 4
Selected bond lengths and angles of compound **3**

Bond lengths (Å)		Bond angles (°)	
Fe(1)–N(2)	1.916(4)	N(2)–Fe(1)–N(6)	175.4(2)
Fe(1)–N(6)	1.928(5)	N(2)–Fe(1)–N(5)	102.2(2)
Fe(1)–N(5)	1.980(5)	N(6)–Fe(1)–N(5)	81.6(2)
Fe(1)–N(1)	1.984(5)	N(2)–Fe(1)–N(1)	81.1(2)
Fe(1)–S(2)	2.201(19)	N(6)–Fe(1)–N(1)	101.9(2)
Fe(1)–S(1)	2.225(19)	N(5)–Fe(1)–N(1)	86.8(2)
S(1)–C(13)	1.749(6)	N(2)–Fe(1)–S(2)	91.06(15)
N(2)–C(1)	1.309(7)	N(6)–Fe(1)–S(2)	85.55(16)
N(2)–N(3)	1.358(6)	N(5)–Fe(1)–S(2)	165.38(15)
Fe(2)–Cl(4)	2.156(2)	N(1)–Fe(1)–S(2)	89.13(16)
Fe(2)–Cl(3)	2.168(2)	N(2)–Fe(1)–S(1)	85.30(15)
Fe(2)–Cl(2)	2.171(2)	N(6)–Fe(1)–S(1)	92.03(15)
Fe(2)–Cl(1)	2.196(2)	N(5)–Fe(1)–S(1)	90.19(16)
C–H···π	H···Cg (Å)	X···Cg (Å)	X–H···Cg (°)
C12–H12···Cg(4)[a]	2.7053	3.1962	113.95
C29–H29···Cg(3)[a]	2.7790	3.1651	104.77
H-bonding interactions	H···A (Å)	D···A (Å)	D–H···A (°)
O1–H102···O2[b]	0.94	2.0425	131
O2–H103···O1[c]	1.70	2.3247	128
O1–H104···O2[d]	1.65	2.3247	122
C14–H14A···S2	2.78	3.6489	145

Cg(3) = Fe1, N1, C8, C1, N2, Cg(4) = Fe1, N5, C25, C18, N6.

[a] x, y, z.

[b] $2 - x, 1 - y, -z$.

[c] $1 + x, 1 + y, z$.

[d] $1 - x, 1 - y, -z$.

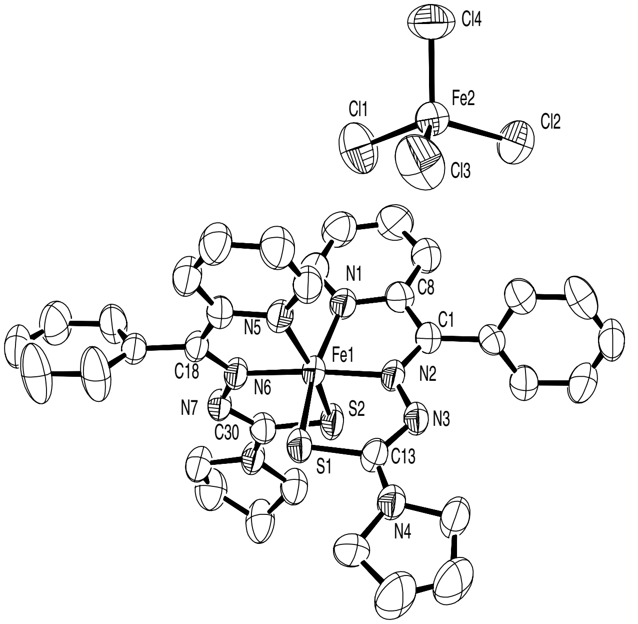

Fig. 2. ORTEP diagram of the compound[Fe(BpypTsc)$_2$]FeCl$_4$ · 2H$_2$O (**3**) with 50% ellipsoidal probability. Hydrogen atoms and lattice water molecules are omitted for clarity.

late rings. The crystallographic asymmetric unit contains a [Fe(BpypTsc)$_2$] cation and a tetrachloroferrate (FeCl$_4^-$) anion along with two molecules of lattice water.

Coordination lengthens the ligands C13–S1 and C1–N2 bonds to 1.749 and 1.309 Å, respectively, and this is an explicit indication of the deprotonation followed by the coordination of the ligand moiety. There is a slight shortening of the Fe–N(azomethine) bond distance compared to Fe–N(py) distances; this may be attributed to the fact that the azomethine nitrogen is a stronger base compared with the pyridyl nitrogen. The two azomethine nitrogen atoms are *trans* to each other, while the pyridyl nitrogen atoms and thiolato sulfur atoms are in *cis* positions. The ligands are orthogonal to the metal ion, with the NNS coordination in a meridonal fashion [24]. The chelate rings are almost planar. There exist strong C–H$\cdots\pi$ interactions between these metal containing chelate rings Cg(3) and Cg(4) with pyridyl ring protons. The tetrachloroferrate anion present in the molecule is slightly distorted tetrahedral with equal bond lengths (~2.187 Å) and angles (~109.46°).

3.4. IR spectra

In Table 5 we have compiled the assignments of IR bands most useful for the establishment of the mode of coordination of thiosemicarbazone ligands in their iron(III) coordination. Coordination of the azomethine nitrogen is indicated by the lowering of the band at 1630 cm^{-1} by 30–50 cm^{-1}. The band is not a pure vibrational band of C=N stretching, but it is a combination band of C=C vibrations of the pyridyl ring also [25]. Two bands ≈1340 and 840 cm^{-1} were assigned to the C–S stretching and bending mode of vibrations. These bands also shift to lower energies in all complexes compared to the ligand, indicating the coordination of the thiolato sulfur. Another band which is considered to be sensitive to coordination is ν(N–N) which is raised in energy due to coordination because of the increased double bond character. The newly formed C=N bond due to the deprotonation of the ligand is also observed ≈1630 cm^{-1}. The spectra of the complexes showed an increase in pyridyl ring in-plane and out-of-plane bending mode of vibrations at ≈440 and 650 cm^{-1}.

Table 6 shows the polyatomic anionic vibrations along with the M–L stretching vibrations observed in the far-IR and IR regions. Fig. 3 shows the far-IR spectra of the complexes. The spectra of compound **1**

Table 5
Ligand vibrational data of the complexes

Compound	ν(C=N)	ν(N=C)	ν(N=N)	ν/δ(C=S)
HBpypTsc	1630 s		1118 s	1342 s, 842 w
[Fe(BpypTsc)$_2$]ClO$_4$ (**1**)	1594 s	1627 s	1163 s	1240 m, 843 w
[Fe(BpypTsc)$_2$]NO$_3$ (**2**)	1594 s	1628 s	1108 s	1202 s, 839 w
[Fe(BpypTsc)$_2$]FeCl$_4$ (**3**)	1595 m	1645 m	1111 s	1204 s, 844 w

All values are in cm^{-1}.

Table 6
Far-IR and anionic vibrational data of the complexes

Compound	ν(Fe–N$_{azo}$)	ν(Fe–N$_{py}$)	ν(Fe–S)	ν(X^a)
[Fe(BpypTsc)$_2$]ClO$_4$ (**1**)	515 w	354 w	452 w	470 w, 1105 s, 619 w
[Fe(BpypTsc)$_2$]NO$_3$ (**2**)	585 w	364 w	450 w	698 w, 839 w, 1379 s, 1289 s
[Fe(BpypTsc)$_2$]FeCl$_4$ (**3**)	528 w	352 s	419 s	374 s, 320 s, 134 w, 110 s

All values are in cm^{-1}.
[a] ClO$_4$, FeCl$_4$, NO$_3$.

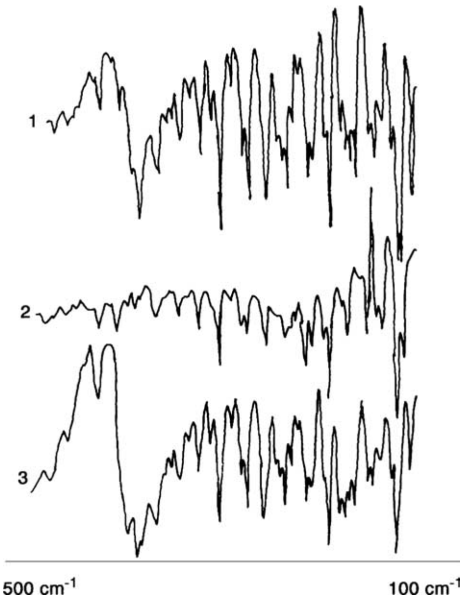

Fig. 3. Far-IR spectra of the iron(III) complexes.

had broad split bands assignable to $\nu_3(ClO_4) \approx 1105$ cm^{-1}, it is unlikely that the perchlorate ion is bound directly to the iron(III) centre since there is no indication of splitting of $\nu_4(ClO_4) \approx 619$ cm^{-1}. This is also confirmed by the absence of $\nu_1(ClO_4) \approx 920$ cm^{-1}. Besides these $\nu_2(ClO_4)$ is also observed ≈470 cm^{-1}. All these bands are split due to the strong H-bonding interactions in the molecule [26]. A similar splitting occurs in the $\nu_3(FeCl_4) \approx 374$ cm^{-1} band in the spectrum of compound **3**. This splitting may be due to the steric factors which reduce the symmetry from tetrahedral [27]. Similarly the band corresponding to $\nu_4 \approx 134$ cm^{-1} is also found to be split due to site effects. The other two stretching modes ν_1 and ν_2 are found at approximately 330 and 114 cm^{-1}, respectively, in the spectrum of compound **3**. The spectrum of compound **2** has two strong bands at 1389 and 1289 cm^{-1} corresponding to ν_1 and ν_4 of the nitrato group. The absence of a combination band ≈1740 cm^{-1} assignable to $\nu_1 + \nu_4$ indicates the ionic nature of the group [28]. Bands at ≈515 and 355 cm^{-1} are assigned to the Fe–N vibrations of the azomethine and pyridyl nitrogen coordination, respectively. Fe–S bond stretching vibrations are found approximately at 420 cm^{-1} in the spectra of the complexes.

3.5. Electronic spectra

Table 7 shows the electronic spectral values in solid-state DRS mode. Fig. 4 shows the electronic spectrum of compound **3**. The UV region is dominated by two intense intra ligand bands at ~36 000 and 29 000 cm^{-1} assigned to $\pi \rightarrow \pi^*$ and $n \rightarrow \pi^*$ transitions.

Usually $n \rightarrow \pi^*$ transitions involving N and S atoms occur at a lower energy than $\pi \rightarrow \pi^*$. Bands which are between 36 000 and 30 000 cm^{-1} in the spectrum of the complexes having pyridyl ligands have been assigned to $\pi \rightarrow \pi^*$ and $n \rightarrow \pi^*$ transitions and the bands between 15 000 and 27 000 cm^{-1} are assigned to $d \rightarrow \pi^*$ transitions, S → Fe and other ligand-to-metal charge transfer transitions. The bands below 15 000 cm^{-1} are due to d → d bands which correspond to a $^2T_{2g} \rightarrow {}^2T_{1g}$ transition of the d^5 spin-paired systems [29]. A comparison of the spectra of **1**, **2** and **3** shows no significant differences indicating that electronic spectra of the cations dominate the spectral properties [30]. Therefore the spin forbidden transitions between 13 700 and 16 600 cm^{-1} of $[FeCl_4]^-$ are too weak to be observed. Unfortunately the electronic spectra of low-spin iron(III) compounds have not been adequately characterized.

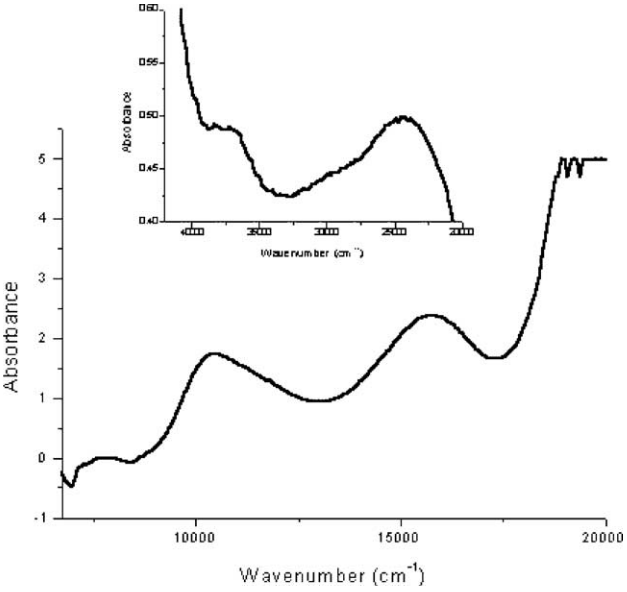

Fig. 4. UV–Vis-NIR spectrum of compound 3 (insight: UV region).

Table 7
Electronic spectral data of the complexes

Compound	$\pi \rightarrow \pi^*$	$n \rightarrow \pi^*$	LMCT	d → d
HBpypTsc	43 300	29 240, 29 760	–	–
$[Fe(BpypTsc)_2]ClO_4$ (**1**)	36 5136	30 487	26 737, 15 503	10 362
$[Fe(BpypTsc)_2]NO_3$ (**2**)	36 630	29 585	24 509, 15 822	10 373
$[Fe(BpypTsc)_2]FeCl_4$ (**3**)	37 037	30 211	24 390, 211 416, 15 974	10 438

All values are in cm^{-1}.

3.6. Electron paramagnetic resonance spectra

The EPR spin Hamiltonian parameters of the iron(III) complexes obtained after the spectral simulations performed by EasySpin package [31] are presented in Table 8. Figs. 5–7 show the EPR spectra of the complexes recorded under different conditions. The EPR of the d^5 iron(III) is expressed by the spin Hamiltonian [32,33],

$$H = \beta[g_x H_x \cdot S_x + g_y H_y \cdot S_y + g_z H_z \cdot S_z]$$

with $S = 1/2$ and $g = 2.00$.

The polycrystalline EPR spectra of compound **3** consist of a single broad line with a Δpk (peak-to-peak) value $\sim$27 mT and a comparatively higher g value $\sim$2.25. This feature does not change even when the temperature is lowered to 100 K. This is indicative of the presence of a mixture of spin species in the system. The observed g value $\approx$2.0 and a nearly isotropic spectra indicate spin–spin relaxation via dipole–dipole interactions. However the solid-state spectra of the other two compounds **1** and **2** are rhombic in nature with three g values. This type of feature is common for low spin octahedral complexes [34]. The observed anisotropic character is due to rhombic distortion common for spin paired iron(III) complexes.

The isotropic spectrum of complex **3** in the polycrystalline state changes to a rhombic spectrum in frozen solution in DMF. Since the g_{av} values obtained at both temperatures are similar, it is likely that lattice effects in the solid state may account for this change from isotropic to rhombic and it is common for spin paired iron(III) complexes. The small deviation of the anisotropic g values from 2.0 suggests that the unpaired electron is in the d_{xy} orbital with a $d_{xz}^2 d_{yz}^2 d_{xy}^1$ ground state configuration. It was interesting to note a sharp but small signal corresponding to $g = 4.2603$ indicating the presence of a high spin species which was identified as the $[FeCl_4]^-$ anion. The spectra of the compounds **1** and **2** recorded in dichloromethane at 100 K also show anisotropic spectra with three g values corresponding to a low spin octahedral iron(III) system. However the spectral features were not resolved probably due to poor glass formation.

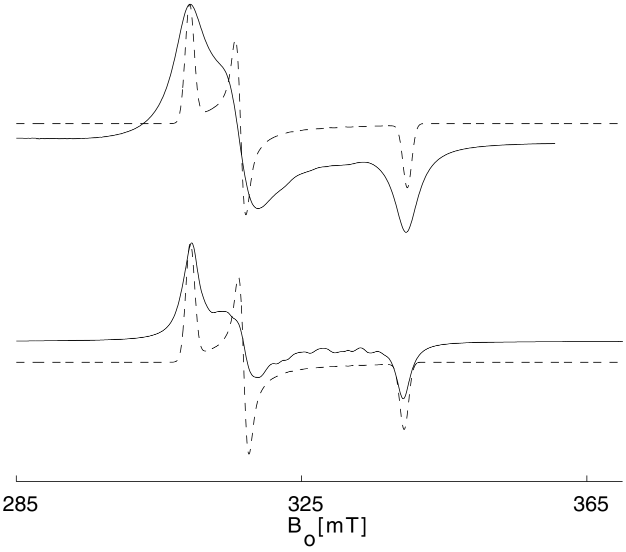

Fig. 5. EPR spectrum of compound **1** in the polycrystalline state: upper trace at 298 K, lower trace at 100 K. Dotted lines shows the simulated best fit spectra of the compound.

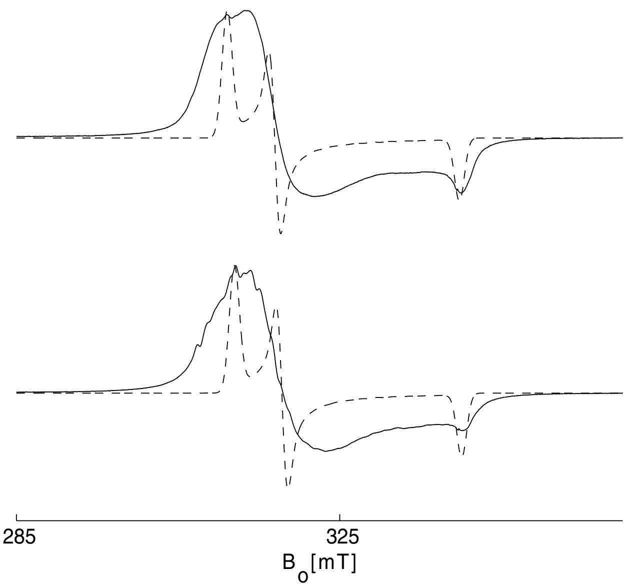

Fig. 6. EPR spectrum of compounds **1** and **2** in a solution of dichloromethane at 100 K: upper trace compound **1**, lower trace compound **2**. Dotted lines show the simulated best fit spectra of the compounds.

Table 8
EPR spectral data of the complexes

Compound	State	Temperature (K)	g_1	g_2	g_3
$[Fe(BpypTsc)_2]ClO_4$ (**1**)	powder	298	2.1990	2.1495	2.0026
	powder	100	2.1984	2.1466	2.0052
	CH_2Cl_2	100	2.1803	2.1400	2.0010
$[Fe(BpypTsc)_2]NO_3$ (**2**)	powder	298	2.1899	2.1465	2.0036
	powder	100	2.1897	2.1462	2.0032
	CH_2Cl_2	100	2.1866	2.1460	2.0027
$[Fe(BpypTsc)_2]FeCl_4$(**3**)	powder	298			2.2594, $\Delta pk = 30$ mT
	powder	100			2.1490, $\Delta pk = 27$ mT
	DMF	100	2.1935	2.1432	1.9981, 4.2603

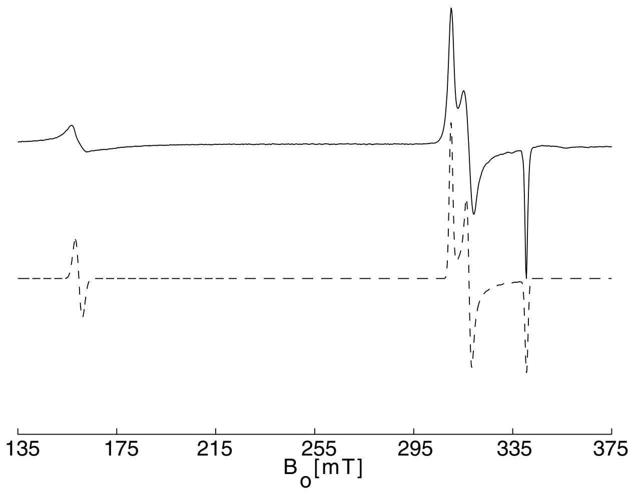

Fig. 7. EPR spectrum of compound **3** in a solution of DMF at 100 K: upper trace experimental spectrum, lower trace simulated best fit spectrum.

3.7. Mössbauer spectra

Mössbauer spectra of the complexes were recorded at 298 and 20 K in order to understand and confirm the spin behavior of the systems. The Mössbauer parameters calculated from the spectra are presented in Table 9, and Figs. 8–10 show the spectra of the complexes. All values were compared with α-iron as a standard.

The high intensity doublet in the spectra of all the complexes with an isomer shift approximately at −0.12 mm s^{-1}, characterized by a quadrupolar splitting $\Delta E_q \approx 2.1$ mm s^{-1}, is ascribed to the low spin $^2T_{2g}$ ground state of low spin iron(III) [35]. These values change a little when the temperature is lowered. The signals in the low temperature spectra were more intense. The 1:1 ratio between the quadrupole split spectra is not strictly observed due to the anisotropic absorption known as the Goldansky–Karyagin effect. The spectra of compound **3** is unusually interesting with the presence of another broad signal corresponding to $\delta^{is} \approx 0.12$ mm s^{-1} $\Delta E_q \approx 0.67$ mm s^{-1}, ascribed to a tetrahedral high spin iron(III) species [36]. The observation of the broad line with unresolved quadrupolar splitting is assumed to be due to much slower spin relaxation due to the orbital electrons of iron. The high spin signal is temperature dependent and in the 20 K spectrum of compound **3** the signal is found to be shifted compared to the 298 K spectrum, and it was found to be more intensified. There are no changes between the 298 and 20

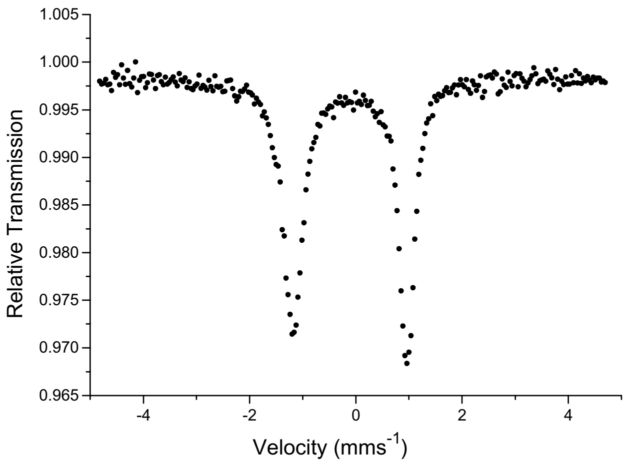

Fig. 8. Mössbauer spectrum of compound **1** (298 K).

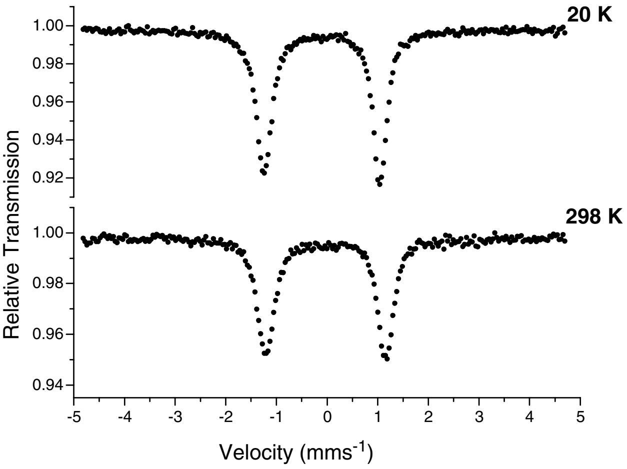

Fig. 9. Mössbauer spectra of compound **2** at different temperatures.

Table 9
Mössbauer spectral data of the complexes

Compound	Temperature (K)	Spin	δ^{is} (mm s^{-1})	ΔE_q (mm s^{-1})
$[Fe(BpypTsc)_2]ClO_4$ (**1**)	298	1/2	−0.17 ($^2T_{2g}$)	2.231 ($^2T_{2g}$)
$[Fe(BpypTsc)_2]NO_3$ (**2**)	298	1/2	−0.11 ($^2T_{2g}$)	2.351 ($^2T_{2g}$)
	20	1/2	−0.12 ($^2T_{2g}$)	2.352 ($^2T_{2g}$)
$[Fe(BpypTsc)_2]FeCl_4$ (**3**)	298	1/2	−0.10 ($^2T_{2g}$)	2.110 ($^2T_{2g}$)
	20	1/2	−0.11 ($^2T_{2g}$)	2.241 ($^2T_{2g}$)
	298	5/2	0.17 ($^6A_1$)	0.925 ($^6A_1$)
	20	5/2	0.12 ($^2T_{2g}$)	0.625 ($^2T_{2g}$)

All values are relative to α-iron.

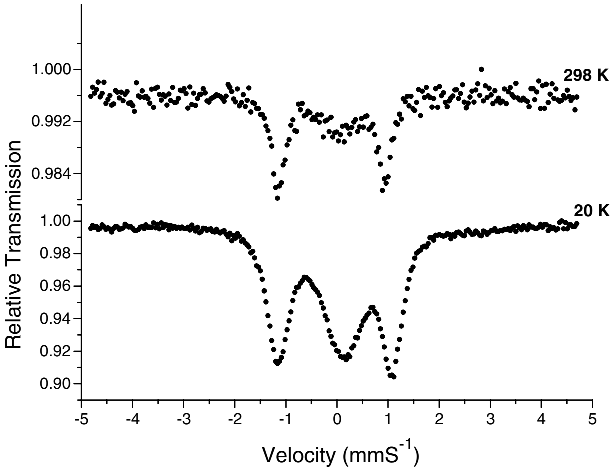

Fig. 10. Mössbauer spectra of compound **3** at different temperatures.

K spectra of the signal due to the spin-paired iron moiety showing the presence of a stable spin system without any magnetic interactions in the molecules [37].

3.8. Supplementary information

Crystallographic data for the structural analysis has been deposited with the Cambridge Crystallographic Data centre, CCDC 217178 for compound HBpypTsc and CCDC 217177 for compound [Fe(BpypTsc)$_2$]-FeCl$_4 \cdot 2$H$_2$O (**3**). Copies of this information may be obtained free of charge from The Director, CCDC, 12 Union Road, Cambridge, CB2 IEZ, UK (fax: +44-1223-336-033; E-mail: deposit@ccdc.cam.ac.uk or http://www.ccdc.cam.ac.uk).

Acknowledgements

One of the authors (A.S.) thanks the Cochin University of Science and Technology for a Research Fellowship. The authors are thankful to the National Single Crystal X-ray Diffraction Facility, IIT, Bombay for the X-ray diffraction studies and Dr. Ajay Gupta, Inter-university Consortium, Indore, India for Mössbauer spectral experiments. M.R.P. Kurup is thankful to the Science, Technology and Environment Department (STED), Govt. of Kerala for financial assistance.

References

[1] M.J. Nelson, H. Jin, I.M. Turner Jr., G. Grove, R.C. Scarrow, B.A. Brennan, L. Que Jr., J. Am. Chem. Soc. 113 (1991) 7072.
[2] R.C. Scarrow, B.A. Brennan, J.G. Cummings, H. Jin, D.J. Duong, J.T. Kindit, M.J. Nelson, Biochemistry 35 (1996) 100078.
[3] T. Bessel, K.S. Burger, G. Vogit, K. Wieghardt, C. Butzlaff, A.X. Trautwein, Inorg. Chem. 32 (1993) 124.
[4] J.C. Noveron, R. Herradora, M.M. Olmstead, P.K. Mascharak, Inorg. Chim. Acta 282 (1999) 269.
[5] A.E. Liberta, D.X. West, Biometals 5 (1992) 121.
[6] R. Raina, T.S. Srivastava, Inorg. Chim. Acta 67 (1982) 83.
[7] R.P. John, A. Sreekanth, M.R.P. Kurup, S.M. Mobin, Polyhedron 21 (2002) 2515.
[8] R.P. John, A. Sreekanth, M.R.P. Kurup, A. Usman, I.A. Razak, H.K. Fun, Spectrochim. Acta A 59 (2003) 1349.
[9] A. Sreekanth, S. Sivakumar, M.R.P. Kurup, J. Mol. Struct. 655 (2003) 47.
[10] A. Sreekanth, M.R.P. Kurup, Polyhedron 22 (2003) 3321.
[11] P. Bindu, M.R.P. Kurup, T.R. Satyakeerthy, Polyhedron 18 (1999) 321.
[12] B.S. Garg, M.R.P. Kurup, S.K. Jain, Y.K. Bhoon, Transition Met. Chem. 13 (1988) 247.
[13] B.S. Garg, M.R.P. Kurup, S.K. Jain, Y.K. Bhoon, Synth. React. Inorg. Met.- Org. Chem. 28 (1998) 1415.
[14] Y.K. Bhoon, J.P. Scovill, D.L. Klayman, Transition Met. Chem. 7 (1982) 264.
[15] J.P. Scovill, Phosphorous Sulfur Silicon Relat. Elem. 60 (1991) 15.
[16] G.M. Sheldrick, Program for the Solution of Crystal Structures, University of Göttingen, Göttingen, Germany, 1997.
[17] G.M. Sheldrick, Program for the Solution of Crystal Structures, University of Göttingen, Göttingen, Germany, 1997.
[18] W.J. Geary, Coord. Chem. Rev. 7 (1971) 81.
[19] S.A. Cotton, Coord. Chem. Rev. 8 (1978) 185.
[20] N.C. Saha, A. Saha, R.J. Butcher, S. Chaudhuri, N. Saha, Inorg. Chim. Acta 339 (2002) 348.
[21] S. Vasudevan, H.N. Vasan, C.N.R. Rao, Chem. Phys. Lett. 65 (1979) 444.
[22] A. Usman, I.A. Razak, S. Chantrapromma, H.K. Fun, V. Philip, A. Sreekanth, M.R.P. Kurup, Acta Crystallogr., Sect. C. Cryst. Struc. Commun. C 58 (2002) o652.
[23] N.C. Saha, R.J. Butcher, S. Chaudhari, N. Saha, Polyhedron 22 (2003) 375.
[24] A. Usman, I.A. Razak, S. Chantrapromma, H.K. Fun, A. Sreekanth, S. Sivakumar, M.R.P. Kurup, Acta Crystallogr., Sect. C. Cryst. Struct. Commun. C 58 (2002) m461.
[25] D.X. West, P.M. Ahrweiler, G. Ertem, J.P. Scovill, D.L. Klayman, J.L.F. Anderson, R. Gilardi, C. George, L.K. Pannel, Transition Met. Chem. 10 (1985) 264.
[26] K. Nakamoto, Infrared and Raman Spectra of Inorganic and Coordination Compounds, 5th ed., Wiley, New York, 1997.
[27] J.S. Avery, C.D. Burbridge, D.M.L. Goodgame, Spectrochim. Acta, Part A 24 (1968) 1721.
[28] I. Nakagwa, J.L. Walter, J. Chem. Phys. 51 (1969) 1389.
[29] A.H. Ewald, R.L. Martin, E. Sinn, A.H. White, Inorg. Chem. 8 (1968) 1837.
[30] E. Konig, K. Madeja, Spectrochim. Acta Part A 23 (1967) 45.
[31] St. Stoll, Spectral simulations in solid-state EPR, PhD Thesis, ETH, Zurich, 2003.
[32] B. Bleaney, M.C.M. O'Brien, Proc. Phys. Soc. London Sect. B 69 (1956) 1216.
[33] J.S. Griffith, The Theory of Transition Metal Ions, Cambridge University Press, London, 1961.
[34] Y. Nishida, A. Sumita, K. Hayashida, H. Olishima, S. Kida, Y. Maedo, J. Coord. Chem. 9 (1979) 261.
[35] S. Floquet, M.L. Boillot, E. Riviere, F. Varret, K. Boukheddaden, D. Morineau, P. Negrier, New. J. Chem. 27 (2003) 341.
[36] N.A. Bell, J.S. Brooks, J.K. Robinson, S.C. Thrope, J. Chem. Soc., Faraday Trans. 94 (1998) 3155.
[37] A.G. Maddock, Mössbauer Spectroscopy, Principles and Applications of the Techniques, Ellis Horwood, Chichester, 1997.